

On numerical treatment of large elastic-viscoplastic deformations

K. -D. KLEE and J. PAULUN (HANNOVER)

MATERIAL equations for elastic-viscoplastic behaviour are discussed following the papers of Bingham, Hohenemser, Prager and Perzyna. For the numerical treatment the flow rule of Perzyna is modified. It can be shown that the given rule leads to the well-known Von Mises flow rule as a limit case. For moderately large rotations and strains of a solid a special incremental form of principle of virtual work is given in Lagrangean description. Green's strain tensor and the second Piola-Kirchhoff stress tensor are used. The coupled physical and geometrical nonlinearities are described and an incremental form for the elastic-viscoplastic material equation is formulated. Some critical remarks on the numerical solution for elastic-plastic deformations by an elastic-viscoplastic algorithm are given. Plane stress problems, e.g. a perforated strip, are calculated numerically using triangular finite elements with quadratic displacement functions.

Na podstawie prac Bingham, Hohenemsera, Pragera i Perzyny omówiono równania konstytutywne dla ciał sprężysto-lepkoplastycznych. Dla zastosowania metod numerycznych zmodyfikowano prawo płynięcia Perzyna. Można wykazać, że prawo to prowadzi w przypadku granicznym do znanego prawa Von Misesa. Dla umiarkowanie dużych obrotów i odkształceń ciała stałego podano w opisie Lagrange'a zasadę prac wirtualnych w specjalnej postaci przyrostowej. Zastosowano tensor odkształcenia Greena i drugi tensor naprężenia Piolięgo-Kirchhoffa. Opisano sprzężenie nieliniowości fizycznych i geometrycznych i sformułowano postać przyrostową równań stanu dla materiałów sprężysto-lepkoplastycznych. Podano pewne uwagi krytyczne dotyczące rozwiązań numerycznych dla ciał sprężysto-plastycznych na podstawie algorytmu dla ciał sprężysto-lepkoplastycznych. Przykład obliczeń numerycznych dotyczy płaskiego stanu naprężenia dla perforowanego pasma rozwiązywanego za pomocą trójkątnych elementów skończonych z kwadratowymi funkcjami przemieszczeń.

На основе работ Бингема, Хохенемсера, Прагера и Перзина обсуждены определяющие уравнения для упруго-вязкопластических тел. Для применения численных методов модифицирован закон течения Перзина. Можно показать, что этот закон приводит в предельном случае к известному закону Мизеса. Для умеренно больших вращений и деформаций твердого тела приведен, в описании Лагранжа, принцип виртуальных работ в специальном виде в приростах. Применен тензор деформации Грина и второй тензор напряжения Пиоли-Кирхгоффа. Описано сопряжение физических и геометрических нелинейностей и сформулирован вид в приростах уравнений состояния для упруго-вязкопластических материалов. Даются некоторые критические замечания, касающиеся численных решений для упруго-пластических тел на основе алгоритма для упруго-вязкопластических тел. Пример численных расчетов касается плоского напряженного состояния для перфорированной полосы решаемой при помощи треугольных конечных элементов с квадратичными функциями перемещений.

1. Introduction

THE IDEA of describing plastic material behaviour by a viscoplastic flow rule is of recent date. It was created in search of new application domains for the method of finite elements. The first developments in the study of viscoplastic problems were laid by BINGHAM [1] and HOHENEMSER, PRAGER [2]. Further developments of the idea of Hohenemser, Prager were given by MALVERN [3] and PERZYNA [4]. The numerical treatment of viscoplastic

materials was carried out by ZIENKIEWICZ, CORMEAU [5], CORMEAU [6] and NAGARAJAN, POPOV [7]. They showed that the viscoplastic model is physically reasonable and leads to a simple numerical algorithm for the finite element solution of plastic deformations. A theoretical proof of the plastic solution as a viscoplastic limit case for a modified Perzyna flow-rule is given in our paper. Till now the numerical applications were restricted to problems with small deformation gradients, i.e. only geometrical linear cases were calculated. Recently the influence of nonlinear effects has been investigated by KANCHI *et al.* [8]. In our paper the geometrical nonlinearity is treated by using Lagrangean description. For this purpose a special principle of incremental virtual work is formulated, in which all nonlinear terms due to Green's strain tensor are included. The application of the displacement approach in the finite element method leads to a system of nonlinear equations which can be solved by an implicate iteration algorithm.

The external load-time-function can be approximated by a combination of load-time increments up to any desired degree of accuracy. For plastic deformations as a limit case the time iteration at each load step is carried out until no further inelastic deformations take place. In connection with this a critical remark on the so-called "one shot solution" introduced by ZIENKIEWICZ, CORMEAU [5] is given.

2. Constitutive equations

The first flow rules in the developments of viscoplastic stress-strain relations were given by BINGHAM [1] and HOHENEMSER, PRAGER [2]. In 1922 Bingham postulated a flow rule for an ideal fluid:

$$(2.1) \quad \dot{\varepsilon}_{ij}^{vp} = \frac{1}{2\eta} (\sqrt{J_2} - \tau_0) \frac{\sigma'_{ij}}{\sqrt{J_2}}.$$

In this rule the components $\dot{\varepsilon}_{ij}^{vp}$ of the viscoplastic strain rate tensor depend on a fluid constant η , a measure of overstress given by the second invariant J_2 of the stress deviator components σ'_{ij} and a constant static yield stress τ_0 . Later HOHENEMSER, PRAGER [2] formulated an extended stress strain relation including elastic strains and hardening effects, here given for deviatoric strain rates

$$(2.2) \quad \dot{\varepsilon}'_{ij} = \frac{1}{2\mu} \dot{\sigma}'_{ij} + \frac{1}{2\eta} (\sqrt{J_2} - \tau_0 - 2\alpha\sqrt{I_2}) \frac{\sigma'_{ij}}{\sqrt{J_2}}.$$

The hardening is described by the second invariant I_2 of the strain tensor and μ denotes the shear modulus. PERZYNA [4] generalized this rule

$$(2.3) \quad \begin{cases} \dot{\varepsilon}'_{ij} = \frac{1}{2\mu} \dot{\sigma}'_{ij} + \gamma \langle \Phi(F) \rangle \frac{\partial F}{\partial \sigma_{ij}}, \\ \langle \Phi(F) \rangle = \begin{cases} 0 & \text{for } F \leq 0, \\ \Phi(F) & \text{for } F > 0, \end{cases} \end{cases}$$

by introducing the flow function

$$(2.4) \quad F = \frac{\sqrt{J_2}}{\kappa} - 1$$

given for an isotropic hardening material with a hardening parameter κ . With a function Φ and a viscosity parameter γ it is possible to adapt this rule to experimental results. This rule can be treated as a generalized form of the rule by MALVERN [3], which was given for rate sensitive materials.

In the following we focus our attention on materials with isotropic hardening, where the influence of hydrostatic stresses on the inelastic behaviour can be neglected. For F we introduce the Huber-Mises flow condition. This leads to

$$(2.5) \quad \dot{\varepsilon}_{ij}^{vp} = \gamma^* \langle \Phi(\sqrt{J_2} - \kappa) \rangle \frac{\sigma'_{ij}}{\sqrt{J_2}},$$

from which we derive the invariant form

$$(2.6) \quad \sqrt{\dot{I}_2^{vp}} := \sqrt{\frac{1}{2} \dot{\varepsilon}_{ij}^{vp} \dot{\varepsilon}_{ij}^{vp}} = \gamma^* \langle \Phi(\sqrt{J_2} - \kappa) \rangle.$$

According to HOHENEMSER, PRAGER [2], we introduce a more generalized linear relation for the rate of hardening

$$(2.7) \quad \dot{\kappa} = \alpha \sqrt{\dot{I}_2^{vp}}.$$

With Eq. (2.6) this leads to

$$(2.8) \quad \dot{\kappa} = \beta \langle \Phi(\sqrt{J_2} - \kappa) \rangle, \quad \beta := \alpha \gamma^*.$$

With a constant β and $\sqrt{J_2}$ as a time-dependent control value, which can be evaluated as a polynomial time function of finite degree, we get for Eq. (2.8) in the case of a linear function Φ a linear differential equation. For this the solution can be given in the following form:

$$(2.9) \quad \kappa(t) = c \exp(-\beta t) + \sqrt{J_2} - \frac{1}{\beta} \dot{\sqrt{J_2}} + \frac{J}{\beta^2} \ddot{\sqrt{J_2}} - + \dots$$

It can be shown that theory of plasticity for isotropic hardening is achieved as a limit case of viscoplasticity. In this limit case α in Eq. (2.7) is finite, and γ^* (and so β) in Eq. (2.8) tends to infinity and we derive

$$(2.10) \quad \alpha < \infty, \quad \beta \rightarrow \infty \Rightarrow \kappa = \sqrt{J_2}, \quad \dot{\kappa} = \dot{\sqrt{J_2}}$$

which for the linear case is an obvious result of Eq. (2.9). With Eq. (2.6) into Eq. (2.5) and Eq. (2.7) it follows that

$$(2.11) \quad \dot{\varepsilon}_{ij}^{vp} = \sqrt{\dot{I}_2^{vp}} \frac{\sigma'_{ij}}{\sqrt{J_2}} = \frac{\dot{\kappa}}{\alpha} \frac{\sigma'_{ij}}{\sqrt{J_2}}.$$

Using the limit case (2.10) the viscoplastic flow rule can be compared with the well-known plastic flow rule for isotropic hardening material:

$$(2.12) \quad \left. \begin{aligned} \dot{\varepsilon}_{ij}^{vp} &= \frac{1}{\alpha} \frac{\dot{J}_2}{2J_2} \sigma'_{ij} \\ \dot{\varepsilon}_{ij}^p &= \frac{3}{4\zeta\kappa^2} \sigma'_{ij} \sigma'_{mn} \dot{\sigma}_{mn} \end{aligned} \right\}, \quad \alpha = \frac{2}{3} \zeta.$$

As a result the two flow rules are identical and the parameter α is proportional to the plastic tangent modulus ζ derived from the static yield curve. For a nonlinear function Φ the derivation of the limit case is more complicated but leads to the same results.

For large deformations we introduce a linear and isotropic relation between stress- and elastic strain-rates in Lagrangean description

$$(2.13) \quad \dot{S}_{KL} = C_{KLMN} \dot{E}_{MN}^{el},$$

with the Green strain tensor E_{MN} and the second Piola-Kirchhoff stress tensor S_{KL} . In the elasticity tensor

$$(2.14) \quad C_{KLMN} = \frac{\check{C}^*}{1+\nu} \left(\delta_{KM} \delta_{LN} + \frac{\nu}{1-2\nu} \delta_{KL} \delta_{MN} \right),$$

ν denotes the Poisson ratio and with the assumption $\nu = \text{const}$, the Young's modulus \check{C}^* can be determined by the given transformation formula (see Fig. 1), where the first Piola-Kirchhoff comparative stress σ_v and the comparative displacement gradient ε_v are used.

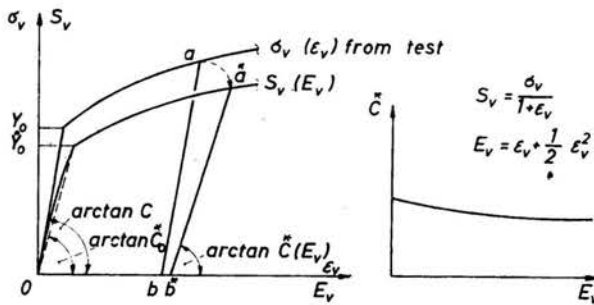


FIG. 1. Transformation of stress-strain curve and Young's modulus \check{C}^* .

The modulus \check{C}^* can be assumed as constant or variable with E_v , (see Fig. 1). For our flow rule we also choose Lagrangean description

$$(2.15) \quad \begin{aligned} \dot{E}_{KL}^{vp} &= \check{\gamma} \langle (\sqrt{J_2} - \kappa) \rangle \frac{S'_{KL}}{\sqrt{J_2}}, \\ J_2 &= \frac{1}{2} S'_{MN} S'_{MN}; \quad \dot{I}_2^{vp} = \frac{1}{2} \dot{E}_{MN}^{vp} \dot{E}_{MN}^{vp}. \end{aligned}$$

In this case the hardening parameter is to be determined by the transformed static stress-strain curve.

3. Principle of incremental virtual work for large displacements

For a material and spatial description Cartesian coordinates with coinciding base vectors are used.

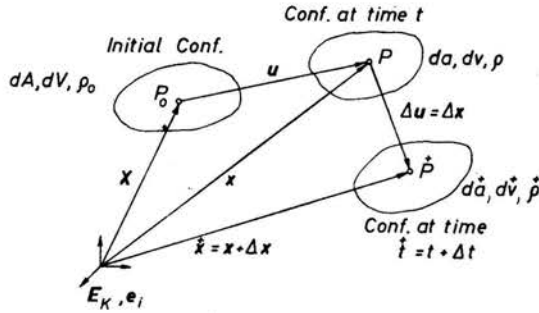


FIG. 2. Configurations of a body.

u denotes the displacement vector and Δu its (finite) increment. For the current configuration at time t the principle of virtual work is stated as

$$(3.1) \quad \int_{(V_0)} S_{KL} \delta E_{KL} dV - \int_{(A_p)} \bar{t}_K \delta u_K dA = 0.$$

In this equation the interior body forces and the inertia body forces are neglected. \bar{t}_K is the vector of the given surface tractions on A_p and with δE_{KL} we denote the virtual Green strain tensor derived from the virtual displacement field δu_K . The same principle holds at time t^+

$$(3.2) \quad \int_{(V_0)^+} \bar{S}_{KL}^+ \delta \bar{E}_{KL}^+ dV - \int_{(A_p)^+} \bar{t}_K^+ \delta \bar{u}_K^+ dA = 0.$$

Time t^+ corresponds to a neighbouring configuration which was reached after a finite time and deformation step from the current configuration. The increments of the displacements, stresses, strains and surface tractions are defined as follows:

$$(3.3) \quad \begin{aligned} \Delta u_K &:= \bar{u}_K^+ - u_K, & \Delta S_{KL} &= \bar{S}_{KL}^+ - S_{KL}, & \Delta t_K^+ &= \bar{t}_K^+ - \bar{t}_K, \\ \Delta E_{KL} &:= \frac{1}{2} (\Delta u_{K,L} + \Delta u_{L,K} + \Delta u_{M,K} u_{M,L} + u_{M,K} \Delta u_{M,L} + \Delta u_{M,K} \Delta u_{M,L}). \end{aligned}$$

The virtual displacement field $\delta \bar{u}_K^+$ in Eq. (3.2) can be reduced to a virtual field $\delta \Delta u_K$ of displacement increments:

$$(3.4) \quad \delta \bar{u}_{KL}^+ = (\delta(u_K + \Delta u_K))_{,L} = \delta \Delta u_{K,L},$$

because the neighbouring configuration is reached by the known current configuration. Then it can be shown that the variation of \bar{E}_{KL}^+ is equal to the variation of the incremental strain tensor. Therefore the principle at time t^+ is simplified to

$$(3.5) \quad \int_{(V_0)} (S_{KL} + \Delta S_{KL}) \delta \Delta E_{KL} dV - \int_{(A_p)} (\bar{t}_K + \Delta \bar{t}_K) \delta \Delta u_K dA = 0.$$

In order to avoid small differences of large numbers in the above expression, we replace in the principle at time t , Eq. (3.1), δu_K by $\delta \Delta u_K$ and so δE_{KL} by

$$(3.6) \quad \delta \Delta E_{KL}^{up} := \frac{1}{2} (\delta \Delta u_{K,L} + \delta \Delta u_{L,K} + \delta \Delta u_{M,K} u_{M,L} + u_{M,K} \delta \Delta u_{M,L});$$

(see PAULUN [9]). Taking this into account and by subtracting Eq. (3.1) from Eq. (3.5), a simplified principle of incremental virtual work

$$(3.7) \quad \int_{(V_0)} \Delta S_{KL} \delta \Delta E_{KL} dV + \int_{(V_0)} S_{KL} \Delta u_{M,K} \delta \Delta u_{M,L} dV - \int_{(A_p)} \Delta \bar{t}_K \delta \Delta u_K dA = 0$$

is achieved.

In the following the proof of the substitution of δu_K by $\delta \Delta u_K$ in the principle at time t is given.

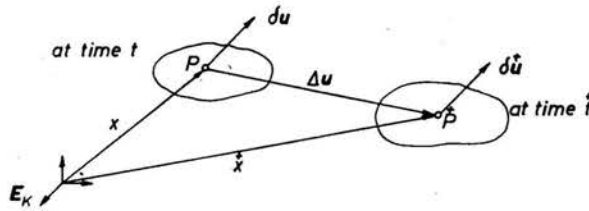


FIG. 3. δu , δu^+ , $\delta \Delta u$ as the admissible virtual displacement field in all configurations.

In Fig. 3 the configurations at time t with an admissible virtual displacement field δu and time t^+ with δu^+ are defined.

With the mappings

$$(3.8) \quad \begin{aligned} \varphi(\mathbf{x}) &= \overset{+}{\mathbf{x}}, & \varphi \in C^1, & \quad \varphi^{-1} \text{ex.}, \\ \psi(\mathbf{x}) &= \delta u, & \overset{+}{\psi}(\overset{+}{\mathbf{x}}) &= \delta u^+, & \overset{++}{\psi} &:= \psi \circ \varphi^{-1} \end{aligned}$$

the following theorem is given:

The set of all mappings $\overset{++}{\psi}$ constructed by admissible ψ is equal to the set of all admissible $\overset{+}{\psi}$,

$$(3.9) \quad \{\overset{++}{\psi} | \psi \text{ adm.}\} = \{\overset{+}{\psi} | \psi^+ \text{ adm.}\}.$$

That means $\overset{++}{\psi}$ delivers an admissible virtual displacement field at time t^+ .

Proof:

- (i) $\overset{++}{\psi}(\overset{+}{\mathbf{x}})$ small:
 $\overset{++}{\psi}(\overset{+}{\mathbf{x}}) = \psi(\varphi^{-1}(\overset{+}{\mathbf{x}})) = \psi(\mathbf{x})$ small (presumption),
- (ii) $\overset{++}{\psi}$ satisfies homogeneous boundary conditions:
 $\overset{+}{A}_u = \varphi(A_u)$ (presumption)
 $\overset{++}{\psi}(\overset{+}{\mathbf{x}})|_{\overset{+}{A}_u} = \psi(\varphi^{-1}(\overset{+}{\mathbf{x}}))|_{A_u} = \psi(\mathbf{x})|_{A_u} = 0,$
- (iii) $\overset{++}{\psi} \in C^1$:
 $\psi, \varphi^{-1} \in C^1$ (presumption)
 $\Rightarrow \overset{++}{\psi} := \psi \circ \varphi^{-1} \in C^1.$

In the proof (ii) the additional presumption was used which claims that the set of material points with geometrical boundary conditions does not change in time.

As a conclusion $\delta \mathbf{u}$ and $\delta \mathbf{u}^+$ are admissible virtual displacement fields at any time. Thus it follows that the difference $\delta \Delta \mathbf{u}$ is also an admissible virtual displacement field at any time.

4. Finite element formulation and solution algorithm

4.1. Finite element description

For the finite element formulation an incremental form of the constitutive equations has to be evaluated:

$$(4.1) \quad E_{KL} := \int_t^{t+\Delta t} \dot{E}_{KL} d\tau \approx \dot{E}_{KL} \Delta t.$$

In Lagrangean representation the additive decomposition of elastic and viscoplastic parts of strain increments are used. With these assumptions the incremental stress-strain relation becomes

$$(4.2) \quad \begin{aligned} \Delta S_{KL} &= C_{KLMN}(\Delta E_{MN} - \Delta t \eta S'_{MN}), \\ \eta &:= \gamma^* \langle \sqrt{J_2} - \kappa \rangle \frac{1}{\sqrt{J_2}}. \end{aligned}$$

Introducing this equation into the principle of incremental virtual work, Eq. (3.7), we get the basic equation for the numerical process:

$$(4.3) \quad \begin{aligned} \int_{(V_0)} \delta \Delta E_{KL} C_{KLMN} \Delta E_{MN} dV - \Delta t \int_{(V_0)} \eta \delta \Delta E_{KL} C_{KLMN} S'_{MN} dV \\ + \int_{(V_0)} S_{KL} \delta \Delta u_{M,K} \Delta u_{M,L} dV - \int_{(A_p)} \Delta \bar{t}_K \delta \Delta u_K dA = 0. \end{aligned}$$

In the finite element formulation the displacements \mathbf{u} are described by a shape function matrix $\mathbf{\Omega}$ and by the vector \mathbf{V} of nodal displacements

$$(4.4) \quad \mathbf{u} = \mathbf{\Omega} \mathbf{V}.$$

By additive splitting of the column matrix $\Delta \mathbf{E}$ of incremental strains, evaluated from Eqs. (3.3)₂ and (4.4),

$$(4.5) \quad \Delta \mathbf{E} = [\mathbf{H} + \mathbf{U}(\mathbf{V})\mathbf{N} + \mathbf{L}(\Delta \mathbf{V})\mathbf{N}]\Delta \mathbf{V},$$

it is possible to calculate geometrically linear or nonlinear cases. In the linear case only the product $\mathbf{H}\Delta \mathbf{V}$ remains. The matrices \mathbf{H} and \mathbf{N} contain derivation terms of the shape function matrix $\mathbf{\Omega}$, the matrices \mathbf{U} and \mathbf{L} depend on the nodal displacement vector \mathbf{V} and, respectively, its increment $\Delta \mathbf{V}$. Introducing Eqs. (4.4) and (4.5) into Eq. (4.3), a system of algebraic equations for the incremental displacements is achieved:

$$(4.6) \quad \begin{aligned} [\mathbf{K}_{el} + \mathbf{K}_{GU}(\mathbf{V}) + \mathbf{K}_{GS}(\mathbf{S}) + \mathbf{K}_{GP}(\mathbf{S}, \Delta t, \eta)]\Delta \mathbf{V} \\ = \mathbf{R}_{el} + \mathbf{R}_p(\mathbf{S}, \Delta t, \eta) + \mathbf{R}_{GP}(\mathbf{V}, \mathbf{S}, \Delta t, \eta) + \mathbf{R}_G(\mathbf{V}, \Delta \mathbf{V}). \end{aligned}$$

4.2. Numerical iteration process

In Eq. (4.6) the matrix of coefficients is decomposed — due to Eq. (4.5) — into an elastic-geometric linear part \mathbf{K}_{el} and additional parts including geometrical nonlinearities (subscript G) and inelastic nonlinearities (subscript P). The same notation is used on the right side of Eq. (4.6). The coefficients depend on the values of the beginning and the end of a time-load step and on the chosen value of a time-load increment.

In order to get a good convergence the nonlinear terms of ΔV are integrated into \mathbf{R}_G on the right side of Eq. (4.6). This system of nonlinear equations can be solved by a numerical iteration process. Such a process can base on the Euler extrapolation rule as an explicit time integration rule. For this rule and in the case of geometrical linearity CORMEAU [6] has developed a condition of stability for the time step

$$(4.7) \quad \Delta t \leq \frac{4(1+\nu)}{\sqrt{3}C\dot{\gamma}^*}$$

By using such a rule, the coefficient matrices in the algebraic equation (4.6), which depend on the current stresses and strains, are constant during a time step interval. This leads to errors in the iteration process. Therefore we introduce the following implicit iteration scheme:

$$(4.8) \quad \begin{aligned} \Delta E^{vpj} &= [\dot{E}_n^{vp}(1-\vartheta) + \dot{E}_{n+1}^{vpj}\vartheta]\Delta t, \\ j = 1: \dot{E}_{n+1}^{vp} &= \dot{E}_n^{vp}, \quad \vartheta \in [0, 1], \end{aligned}$$

n denotes the number of time increments and j the iteration index. For $\vartheta = 0$ the explicit iteration scheme follows. The first iteration step ($j = 1$) is carried out explicitly according to the predictor-corrector method. In the case of geometrical nonlinearity and the explicit iteration scheme, stability is only reached for the half value of Cormeau's time step in Eq. (4.7). The numerical results show us that the implicit scheme is more stable.

In the numerical process the important case of elastic-plastic material is realized by an iteration process with constant load until a state with $\kappa = \sqrt{J_2}$ (see Eq. (2.10)) is reached. The external load can be applied immediately — a so-called "one shot solution" — or in a finite number of load increments as shown in Fig. 4.

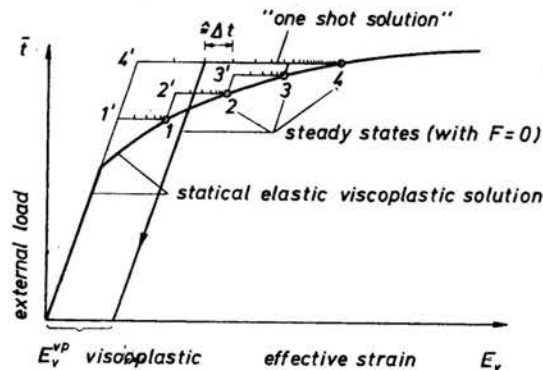


FIG. 4. Iteration processes for elastic-viscoplastic and elastic-plastic deformations.

4.3. Critical remarks on "one shot solution"

In plasticity the final strains depend on the load history. In the "one shot solution" the production of inelastic strains takes place when the external load has been fully applied and so the influence of loading history is excluded. As shown in the example (Fig. 5), the

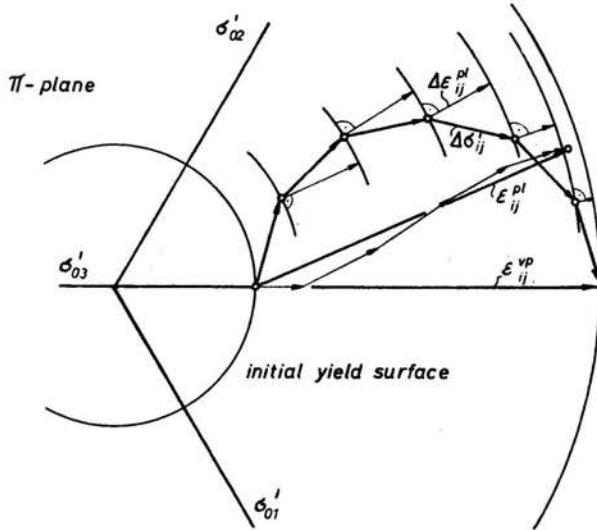


FIG. 5. Different inelastic strain tensor for plastic and "one shot" viscoplastic solution.

final viscoplastic strain tensor has the same direction as the final stress tensor. For the given stress history the final plastic strains which are calculated as the sums of plastic strain increments normal to the current yield surface differ from the viscoplastic strains of "one shot solution". If the affinity in load history is not given, the external load has to be applied in a finite number of increments.

5. Example

A perforated strip under uniaxial tension is investigated using triangular elements with quadratic displacement shape functions (Fig. 6).

The strip consists of an aluminium alloy with strain hardening, idealized by a linear hardening function. For the calculation of the stress distribution a "one shot solution" was used. In Fig. 7 the distribution of nominal stress σ , in the minimum section $B-A$ in dependence of time is given. The steady state can be compared with the measured values of THEOCARIS, MARKETOS [10]. A good agreement of the numerical results with the experimental one can be seen (Fig. 8). In Fig. 9 the final plastic zones for the loads IV ($\bar{t} = 0.4Y_0$) and VI ($\bar{t} = 0.53Y_0$) achieved by the finite element process are compared with the experimental ones.

In the upper part the curves differ more than in the lower one. The reason for that is the relatively rough element subdivision in this region. In Fig. 10 the development of

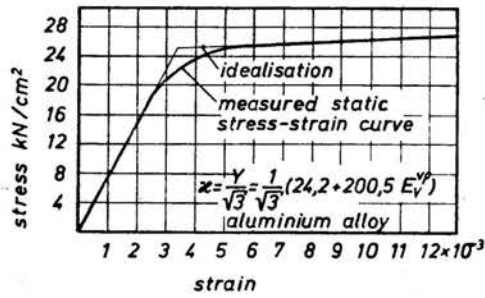
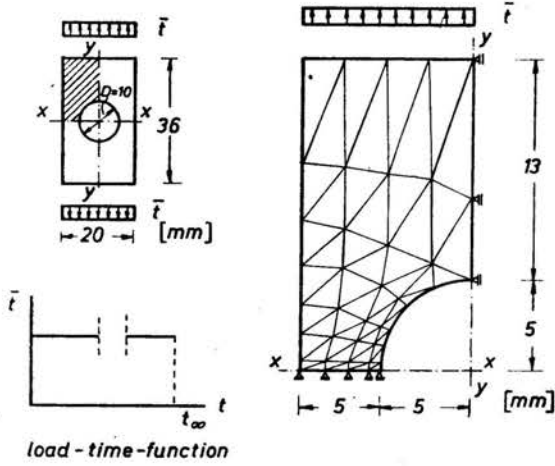


FIG. 6. Perforated strip under tension.

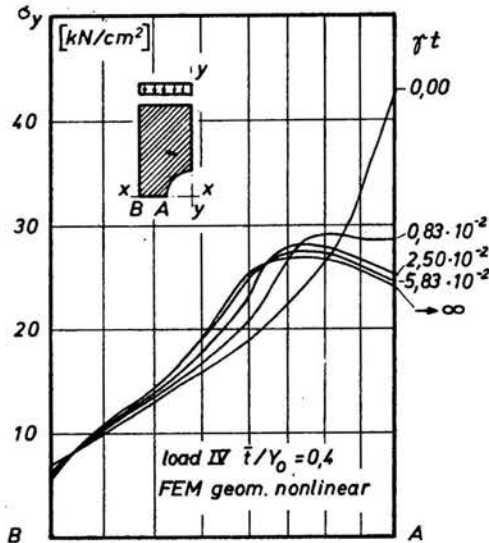


FIG. 7. Distribution of nominal stress σ_y , in dependence of time.

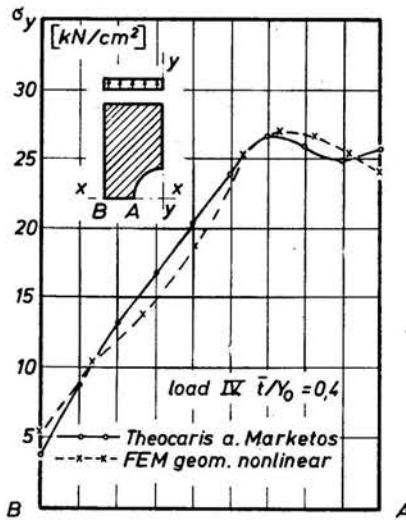


FIG. 8. Distribution of nominal stress σ_y , at steady state.

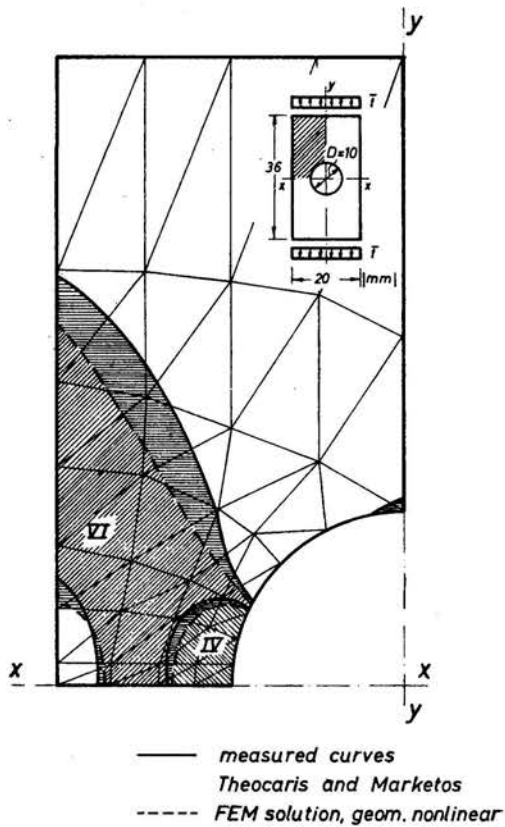


FIG. 9. Comparison of plastic zones.

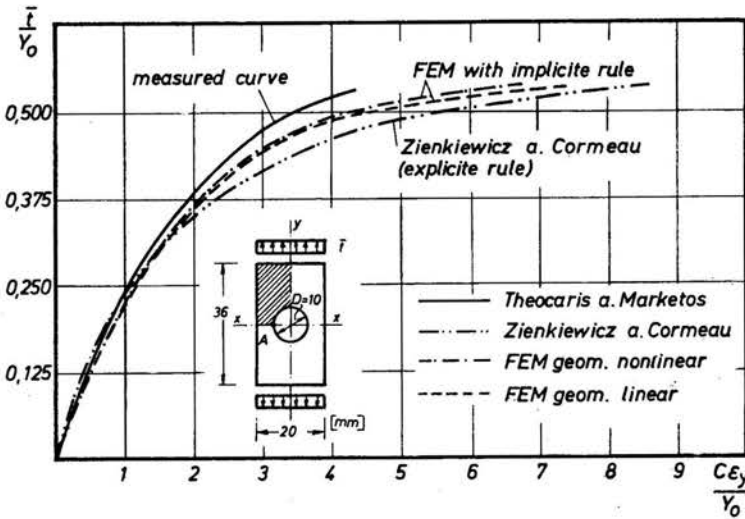


FIG. 10. Measured and calculated maximum displacement gradients ϵ_y for different loads.

the maximum displacement gradient ϵ_y , given as a function of the applied external load, measured by THEOCARIS, MARKETOS [10], is compared with the given finite element calculations based on an implicit and explicit integration rule, respectively. The latter one was achieved by ZIENKIEWICZ, CORMEAU [5] using a geometrically linear calculation.

6. Conclusion

In the given example the influence of geometrical nonlinearity is not remarkable because the displacement gradients are comparatively small. The influence of a geometrical nonlinear calculation increases with growing displacements. The proof that the results of the nonlinear theory are more accurate than those of the linear theory is given by KLEE [11] by using equilibrium conditions.

An advantage of the presented numerical viscoplastic solution algorithm is the flexibility in material description. It is possible to calculate viscoplastic, plastic or creep behaviour with one program. By using this algorithm for plastic material it is not necessary as in the method of initial stress, for example, to fulfill the flow condition after each incremental step. Hence the simulation of an elastic-plastic deformation process by an elastic-viscoplastic solution algorithm is logically simple and numerically most effective.

References

1. E. C. BINGHAM, *Fluidity and plasticity*, Mc Graw-Hill, New York, Chap. VIII, 215-218, 1922.
2. K. HOHENEMSER, W. PRAGER, *Über die Ansätze der Mechanik isotroper Kontinua*, ZAMM, 12, 216-226, 1932.
3. L. E. MALVERN, *The propagation of longitudinal waves of plastic deformation in a bar of material exhibiting a strain-rate effect*, J. Appl. Mech., 18, 203-208, 1951.

4. P. PERZYNA, *Fundamental problems in viscoplasticity*, Adv. Appl. Mech., 243-377, 1966.
5. O. C. ZIENKIEWICZ, I. C. CORMEAU, *Visco-plasticity, plasticity and creep in elastic solids — a unified numerical solution approach*, Int. J. Num. Meth. Eng., 8, 821-845, 1974.
6. I. CORMEAU, *Numerical stability in quasi-static elasto/viscoplasticity*, Int. J. Num. Meth. Eng., 9, 109-127, 1975.
7. S. NAGARAJAN, E. P. POPOV, *Plastic and viscoplastic analysis of axisymmetric shells*, Int. J. Solids Struct., 11, 1-19, 1975.
8. M. B. KANCHI, O. C. ZIENKIEWICZ, D. R. J. OWEN, *The visco-plastic approach to problems of plasticity and creep involving geometric nonlinear effects*, Int. J. Num. Meth. Eng., 12, 169-181, 1978.
9. J. PAULUN, *Zur Theorie und Berechnung geometrisch und physikalisch nichtlinearer Kontinua mit Anwendung der Methode der finiten Elemente*, Forschungs- und Seminarberichte aus dem Bereich der Mechanik der Universität D 3000 Hannover, Bericht F 77/4, 1977.
10. P. S. THEOCARIS, E. MARKETOS, *Elastic-plastic analysis of perforated thin strips of a strain-hardening material*, J. Mech. Phys. Solids, 12, 377-390, 1964.
11. K.-D. KLEE, *Theoretische und numerische Behandlung geometrisch nichtlinearer viskoplastischer Kontinua*, Forschungs- und Seminarberichte aus dem Bereich der Mechanik der Universität D 3000 Hannover, Bericht F 79/1, 1979.

LEHRGEBIET FÜR BAUMECHANIK
UNIVERSITÄT HANNOVER, BRD.

Received August 17, 1979.